

# Quantum chaos, statistical equilibrium and resonant radiative capture of electrons by multicharged ions: $\text{Au}^{24+}$

G. F. Gribakin, A. A. Gribakina, and V. V. Flambaum

*School of Physics, The University of New South Wales, Sydney 2052, Australia*

(September 17, 2018)

## Abstract

We show that the spectrum and eigenstates of open-shell multicharged atomic ions near the ionization threshold are chaotic, as a result of extremely high level densities of multiply excited electron states ( $10^3 \text{ eV}^{-1}$  in  $\text{Au}^{24+}$ ) and a strong configuration mixing. This complexity enables one to use statistical methods to analyze the system. The orbital occupation numbers obey the Fermi-Dirac distribution, and temperature can be introduced. We show that radiative capture of electrons through the multielectron resonant states is strongly enhanced compared to the direct radiative recombination.

PACS numbers: 31.50.+w, 34.80.Lx, 32.70.Cs, 05.30.Fk

In this paper we investigate the spectrum and eigenstates of a multicharged positive ion at energies close to its ionization threshold  $I$ . Using  $\text{Au}^{24+}$  ( $I = 750$  eV) as an example, we show that this spectrum is dominated by multiple electron excitations into a few low-lying unoccupied orbitals. As a result, it is extremely dense, with level spacings  $\sim 1$  meV between the states of a given total angular momentum and parity  $J^\pi$ . The electron Coulomb interaction induces a strong mixing of the multiply-excited configurations, which leads to a statistical equilibrium in the system. The latter is similar to a thermal equilibrium, and variables such as temperature can be introduced to describe it. This enables one to use statistical methods in the situation where a full dynamical quantum calculation is simply impossible because of the enormous size of the Hilbert space ( $\gtrsim 10^5$  for  $\text{Au}^{24+}$ ).

We apply this approach to the problem of radiative capture of low-energy electrons by multicharged positive ions, and show that the contribution of resonant *multielectronic* recombination, which proceeds via electron capture into the multiply-excited compound states, is much greater than that of the direct radiative recombination. Our calculation gives a quantitative explanation of huge enhancements of the recombination rates, and removes the “enormous discrepancies between theoretical and experimental rate coefficients” [1]. The situation here turns out to be similar to the radiative neutron capture by complex nuclei [ $(n, \gamma)$  reaction] where the resonance mechanism involving the compound nucleus states is also much stronger than the direct capture [2].

So far the enhanced recombination at low electron energies  $\lesssim 1$  eV has been observed for a number of ions [3]. Its magnitude ranges from a factor of about ten for  $\text{Ar}^{13+}$ ,  $\text{Au}^{50+}$ ,  $\text{Pb}^{53+}$ , and  $\text{U}^{28+}$  [4], to over a hundred for  $\text{Au}^{25+}$  [1]. This enhancement is sensitive to the electronic structure of the target, e.g., the recombination rates of  $\text{Au}^{49+}$  and  $\text{Au}^{51+}$  are much smaller than that of  $\text{Au}^{50+}$  [4]. For few-electron ions, e.g.,  $\text{C}^{4+}$ ,  $\text{Ne}^{7+}$  and  $\text{Ar}^{15+}$  [5–7], the observed rates are described well by the sum of the direct and dielectronic recombination rates. In more complicated cases, like  $\text{U}^{28+}$  or  $\text{Au}^{25+}$ , the questions of what are the particular resonances just above the threshold and how they contribute to the recombination “remain a mystery” [8].

Let us consider the problem of electron recombination on  $\text{Au}^{25+}$ . Due to electron correlations the electron can be captured into an excited state of the compound  $\text{Au}^{24+}$  ion.  $\text{Au}^{24+}$  has 55 electrons. Its ground state belongs to the  $1s^2 \dots 4f^9$  configuration. Figure 1 shows the energies of its relativistic orbitals  $nlj$  from a self-consistent Dirac-Fock calculation. The energy of the highest orbital occupied in the ground state is  $\varepsilon_{4f_{7/2}} = -29.7$  a.u. Our relativistic configuration-interaction (CI) calculation of the ground states of  $\text{Au}^{24+}4f^9$  and  $\text{Au}^{24+}4f^8$  shows that they are characterized by  $J = \frac{15}{2}$  and 6, and their total energies are  $-18792.36$  and  $-18764.80$  a.u., respectively. Thus, the ionization threshold of  $\text{Au}^{24+}$  is  $I = 27.56$  a.u. = 750 eV.

The excited states of the ion are generated by transferring electrons from the ground state into the unoccupied orbitals above the Fermi level, or into the partially filled  $4f$  orbital. We are interested in the excitation spectrum of  $\text{Au}^{24+}$  near its ionization threshold. This energy (27.5 a.u.) is sufficient to push up a few of the  $4f$  electrons, and even excite one or two electrons from the  $4d$  orbital [9]. Thus, we consider  $\text{Au}^{24+}$  as a system of  $n = 19$  electrons above the inactive Kr-like  $1s^2 \dots 4p^6$  core.

The number of multielectron states obtained by distributing 19 electrons over 31 relativistic orbitals,  $4d_{3/2}$  through to  $7g_{9/2}$ , is enormous, even if we are only interested in the

excitation energies below 27.5 a.u. It is impossible to perform any CI calculation for them. However, there is another simpler way to analyze the spectrum. The scale of the configuration interaction strength is determined by the two-body Coulomb matrix elements. Their typical size in  $\text{Au}^{24+}$  is about 1 a.u., i.e., much smaller than  $I$ . Configuration mixing aside, the CI does not shift the mean energies of the configurations. Therefore, we can construct the excitation spectrum of  $\text{Au}^{24+}$  by calculating the mean energies  $E_i$  of the configurations,

$$E_i = E_{\text{core}} + \sum_a \epsilon_a n_a + \sum_{a \leq b} \frac{n_a(n_b - \delta_{ab})}{1 + \delta_{ab}} U_{ab}, \quad (1)$$

and the numbers of many-electron states in each of them,  $N_i = \prod_a g_a! / [n_a!(g_a - n_a)!]$ , where  $n_a$  are the orbital occupation numbers in the configuration ( $\sum_a n_a = n$ ),  $\epsilon_a$  is the single-particle energy of the orbital  $a$  in the field of the core,  $g_a = 2j_a + 1$ , and  $U_{ab}$  is the average Coulomb interaction between the electrons in orbitals  $a$  and  $b$  (direct – exchange).

We find that there are 9000 configurations within 35 a.u. of the  $\text{Au}^{24+}$  ground state. They comprise a total of  $2.1 \times 10^8$  many-electron states, which corresponds to about  $5 \times 10^5$  states in each  $J^\pi$  manifold. Figure 2 shows the total density of states

$$\rho(E) = \sum_i N_i \delta(E - E_i) \quad (2)$$

averaged over 1 a.u. energy intervals, as a function of  $\sqrt{E}$ , where  $E$  is the excitation energy above the ground state. The inset presents a break-up of the total density near the ionization threshold into the densities of states with given  $J$ :  $\rho(E) = \sum_J (2J + 1) \rho_J(E)$ . The most abundant values are  $J = \frac{5}{2} - \frac{15}{2}$ . For a given parity the density of such states at  $E \approx I$  is  $\rho_{J^\pi} \approx 3.5 \times 10^4$  a.u., which corresponds to a mean level spacing  $D = 1/\rho_{J^\pi} \sim 1$  meV. Figure 2 demonstrates the characteristic  $\rho \propto \exp(a\sqrt{E})$  behaviour of the level density predicted by the Fermi-gas model [10], where  $a$  is related to the single-particle level density at the Fermi level  $g(\varepsilon_F) = 3a^2/2\pi^2$ . A Fermi-gas model ansatz

$$\rho(E) = AE^{-\nu} \exp(a\sqrt{E}), \quad (3)$$

with  $A = 31.6$ ,  $\nu = 1.56$ , and  $a = 3.35$  gives an accurate fit of the level density at  $E > 1$  a.u. The corresponding  $g(\varepsilon_F) = 1.7$  a.u. is in agreement with the orbital spectrum in Fig. 1. For most abundant  $J^\pi$  states  $\rho_{J^\pi}(E)$  is given by Eq. (3) with  $A_{J^\pi} \approx 0.15$ .

At first sight the huge level density makes the  $\text{Au}^{24+}$  problem very complicated. In reality this complexity enables one to use statistical methods to describe the system. The interaction between multiply-excited configuration states mixes them completely, and they lose their individual features. In this regime the spectral statistics are close to those of a random matrix ensemble, the eigenstates cannot be characterized by any quantum numbers except the exact ones (energy and  $J^\pi$ ), and the orbital occupation numbers deviate prominently from integers. This regime can be described as many-body quantum chaos. We have extensively studied it in direct numerical calculations for the rare-earth atom of Ce – a system with four valence electrons [11–13].

The strength of the configuration mixing is characterized by the spreading width  $\Gamma_{\text{spr}}$ . For a configuration basis state  $\Phi_k$  with energy  $E_k$  it defines the energy range  $|E - E_k| \lesssim \Gamma_{\text{spr}}$  of eigenstates in which this basis state noticeably participates. By the same token it shows

that a particular eigenstate  $\Psi = \sum_k C_k \Phi_k$  contains a large number  $N \sim \Gamma_{\text{spr}}/D$  of *principal components* – basis states characterized by  $C_k \sim 1/\sqrt{N}$ . Outside the spreading width  $C_k$  decrease. Apart from this,  $C_k$  behave like random variables [11]. The effect of spreading is approximated well by the Breit-Wigner shape [10]

$$\overline{C_k^2}(E) = N^{-1} \frac{\Gamma_{\text{spr}}^2/4}{(E_k - E)^2 + \Gamma_{\text{spr}}^2/4} . \quad (4)$$

The normalization  $\sum_k \overline{C_k^2} = 1$  yields  $N = \pi\Gamma/2D$ . In systems with small level spacings  $D$  the number of principal components  $N$  can be very large. It reaches several hundreds in Ce, and  $10^6$  in complex nuclei. In Fig. 3 we illustrate this behaviour by the results of a CI calculation for two  $\text{Au}^{24+}$  configurations near the ionization threshold:  $4f_{5/2}^3 4f_{7/2}^3 5p_{1/2} 5p_{3/2} 5f_{7/2}$  and  $4f_{5/2}^3 4f_{7/2}^3 5p_{1/2} 5d_{3/2} 5g_{7/2}$ . These two configurations produce  $1254 J^\pi = \frac{13}{2}^+$  states. Their mixing is complete, since the weight of each configuration in every eigenstate is about 50%. A Breit-Wigner fit of the mean-squared components yields  $N = 975$  and  $\Gamma_{\text{spr}} = 0.50$  a.u. The spreading width is related to the mean-squared off-diagonal Hamiltonian matrix element and the mean level spacing as  $\Gamma_{\text{spr}} \simeq 2\pi \overline{H_{ij}^2}/D$  [10]. When more configurations are included, both  $D$  and  $\overline{H_{ij}^2}$  decrease, and  $\Gamma_{\text{spr}}$  does not change much. If one were able to do a full-scale CI calculation near the ionization threshold of  $\text{Au}^{24+}$  eigenstates with  $N = (\pi/2)\Gamma_{\text{spr}}\rho_{J^\pi} \sim 3 \times 10^4$  would be obtained.

The spreading of the basis states due to configuration interaction introduces a natural statistical averaging in the system. Based on this averaging, a statistical theory of finite Fermi systems of interacting particles can be developed [14]. It enables one to calculate various properties of the system without diagonalizing the Hamiltonian, as sums over the basis states, e.g., the mean occupations numbers,  $n_a(E) = \sum_k \overline{C_k^2}(E) n_a^{(k)}$ , where  $n_a^{(k)}$  is the occupation number of the orbital  $a$  in the basis state  $k$ . Using a simple Gaussian model spreading we calculate mean orbital occupation numbers at different excitation energies. Figure 4 shows that the result (circles) is described well by the Fermi-Dirac formula  $n_a = \{1 + \exp[(\varepsilon_a - \mu)/T]\}^{-1}$ . The temperature  $T$  and the chemical potential  $\mu$  are chosen to give the best fit of the numerical occupation numbers. On the other hand, the temperature can be determined from the level density  $\rho(E)$ , Eq. (2), through the canonical average  $E(T) = Z^{-1} \int e^{-E/T} E \rho(E) dE$ , where  $Z = \int e^{-E/T} \rho(E) dE$ , or from a statistical formula  $T^{-1} = d \ln[\rho(E)]/dE$ , using the smooth fit (3). The latter yields  $T \simeq 2\sqrt{E}/a$ , characteristic of Fermi systems. For energies above 3 a.u. all three definitions give close values, Fig. 5.

Let us now estimate the direct and resonant contributions to the recombination rate of  $\text{Au}^{25+}$ . The direct radiative recombination cross section is estimated by introducing an effective ionic charge  $Z_i$  into the formula of Bethe and Salpeter [15],

$$\sigma^{(d)} = \frac{1.96\pi^2}{c^3} \frac{\text{Ryd}}{\varepsilon} Z_i^2 \ln \left( \frac{Z_i}{n_0} \sqrt{\frac{\text{Ryd}}{\varepsilon}} \right) , \quad (5)$$

where  $\varepsilon$  is the electron energy and  $n_0$  is the principal quantum number of the lowest unoccupied ionic orbital (we use atomic units). Using  $Z_i = 25$ ,  $n_0 = 5$ , and  $\varepsilon = 0.1$  eV we obtain  $\sigma^{(d)} \approx 7 \times 10^{-17}$  cm<sup>2</sup>, which gives a rate of  $\lambda = \sigma v = 1.3 \times 10^{-9}$  cm<sup>3</sup>s<sup>-1</sup>, two orders of magnitude smaller than the experimental  $\lambda = 1.8 \times 10^{-7}$  cm<sup>3</sup>s<sup>-1</sup> at this energy [1].

The energy-averaged cross section of the resonant radiative capture of a low-energy  $s$  electron is [16]

$$\sigma^{(r)} = \frac{\pi^2}{\varepsilon} \frac{\Gamma_\gamma \Gamma_e}{D(\Gamma_\gamma + \Gamma_e)} \approx \frac{\pi^2}{\varepsilon} \frac{\Gamma_\gamma}{D} \quad (\Gamma_e \gg \Gamma_\gamma), \quad (6)$$

where  $\Gamma_\gamma$  and  $\Gamma_e$  are the mean radiative and autoionization (or elastic) widths of the resonances,  $D$  is the mean resonance spacing, and we drop the statistical weights of the initial and intermediate ionic states. The relation  $\Gamma_e \gg \Gamma_\gamma$  is usually valid for a few lower partial waves, where the electron interaction is stronger than the electromagnetic one.

The radiative width of the resonant state at energy  $E \approx I$  is found by summing the partial widths for all lower-lying states  $E' = E - \omega$ ,

$$\Gamma_\gamma \approx \frac{3}{2J+1} \int_0^I \frac{4\omega^3 |d_\omega|^2}{3c^3} \rho_{J\pi}(I-\omega) d\omega, \quad (7)$$

where the factor 3 accounts for  $J' = J, J \pm 1$ , and  $d_\omega$  is the reduced dipole matrix element between the many-electron states. Because of the chaotic structure of these states  $d_\omega$  is suppressed compared to the typical single-particle matrix element  $d_0$ :  $d_\omega \sim d_0/\sqrt{N}$  [2,11,12]. This estimate for systems with dense chaotic spectra in fact follows from the dipole sum rule: the number of lines in the spectrum is large,  $\propto D^{-1} \propto N$ , consequently, the line strengths are small,  $|d_\omega|^2 \sim |d_0|^2 N^{-1}$ .

Using this estimate and calculating the integral in Eq. (7) by the saddle-point method we obtain

$$\sigma^{(r)} = \frac{8\pi d_0^2}{(2J+1)c^3 \varepsilon \Gamma_{\text{spr}}} \sqrt{\frac{2\pi}{3}} \rho_{J\pi}(I-\omega_0) \omega_0^4, \quad (8)$$

where  $\omega_0 = 6\sqrt{I}/a$  corresponds to the maximum of the the decay photon spectrum in Eq. (7). This cross section has the same energy dependence as  $\sigma^{(d)}$ . To evaluate its magnitude we use  $d_0 \sim Z_i^{-1}$ ,  $2J+1 \approx 10$ , and substitute  $\Gamma_{\text{spr}} = 0.5$ ,  $\omega_0 = 9.4$ , and  $\rho_{J\pi}(I-\omega_0) = 2.5 \times 10^3$  a.u. At  $\varepsilon = 0.1$  eV this gives  $\sigma^{(r)} = 7 \times 10^{-16}$  cm<sup>2</sup>, therefore,  $\sigma^{(r)}/\sigma^{(d)} = 10$ , and we obtain a factor of ten enhancement over the direct recombination. It comes from the large effective number of final states in the radiative width in Eq. (7) (numerically  $\Gamma_\gamma \sim 2 \times 10^{-7}$  a.u.). If we include contributions of the higher electron partial waves the enhancement will match the experimentally observed values.

In summary, the resonant radiative capture mechanism fully explains the strongly enhanced recombination rates observed for eV electrons on multicharged ions. Its origin is in the high level densities of chaotic multiply-excited electron states in multicharged ions. The size of the enhancement is sensitive to the electron structure of the ion, which determines the level density. We have shown that a statistical approach can be applied to the analysis of this complex system. One can also use a statistical theory to calculate mean-squared matrix elements between multiply excited chaotic states in terms of single-particle amplitudes, occupation numbers,  $\Gamma_{\text{spr}}$  and  $D$  [11,12,17], and obtain accurate quantitative information about the processes involving chaotic states and resonances. At higher electron energies the resonant capture proceeds via so-called doorway states [10] – simple dielectronic autoionizing states, which are then “fragmented” into the dense spectrum of multiply-excited resonances (see [8] and [12] and Refs. therein).

## REFERENCES

- [1] A. Hoffknecht *et al.*, J. Phys. B **31**, 2415 (1998).
- [2] V. V. Flambaum and O. P. Sushkov, Nuclear Physics **A412**, 13 (1984); **A435**, 352 (1985).
- [3] We do not consider a specific enhancement below 1 meV observed for all ions including the fully stripped Ar<sup>18+</sup>, O. Uwira *et al.*, Hyperfine Interact. **108**, 167 (1997).
- [4] H. Gao *et al.*, Phys. Rev. Lett. **75**, 4381 (1995); O. Uwira *et al.*, Hyperfine Interact. **108**, 149 (1997); A. Müller and A. Wolf, *ibid.* **109**, 233 (1997).
- [5] S. Schennach *et al.*, Z. Phys. D **30**, 291 (1994).
- [6] W. Zong *et al.*, Phys. Rev. A **56**, 386 (1997).
- [7] R. Schuch *et al.*, Phys. Scripta **T73**, 114 (1997).
- [8] D. M. Mitnik *et al.*, Phys. Rev. A **57**, 4365 (1998).
- [9] Infinite Rydberg series belong to the single-particle aspect of the problem, and we do not consider them here.
- [10] A. Bohr and B. Mottelson, *Nuclear structure, Vol. 1* (Benjamin, New York, 1969).
- [11] V. V. Flambaum *et al.*, Phys. Rev. A **50**, 267 (1994).
- [12] V. V. Flambaum, A. A. Gribakina, and G. F. Gribakin, Phys. Rev. A **54**, 2066 (1996); **58**, 230 (1998).
- [13] V. V. Flambaum *et al.*, Phys. Rev. E **57**, 4933 (1998).
- [14] V. V. Flambaum and F. M. Izrailev, Phys. Rev. E **55** R13 (1997); **56** 5144 (1997).
- [15] H. Bethe and E. Salpeter, *Quantum Mechanics of Atoms with One and Two Electrons* (Springer, Berlin, 1957).
- [16] L. D. Landau and E. M. Lifshitz, *Quantum Mechanics*, (Pergamon Press, Oxford, 1977), Ch. 18.
- [17] V. V. Flambaum and O. K. Vorov, Phys. Rev. Lett. **70**, 4051 (1993).

FIGURES

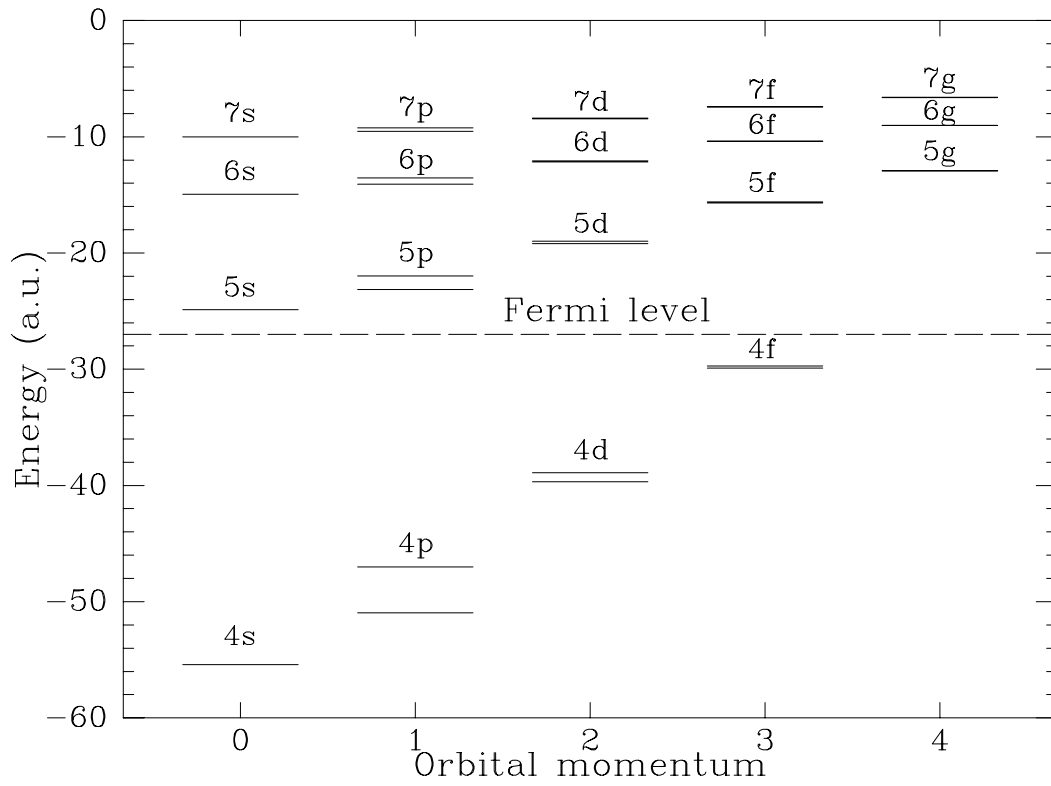


FIG. 1. Electron orbitals of  $\text{Au}^{24+}$  from the Dirac-Fock calculation of its ground state  $1s^2 \dots 4f^9$ .

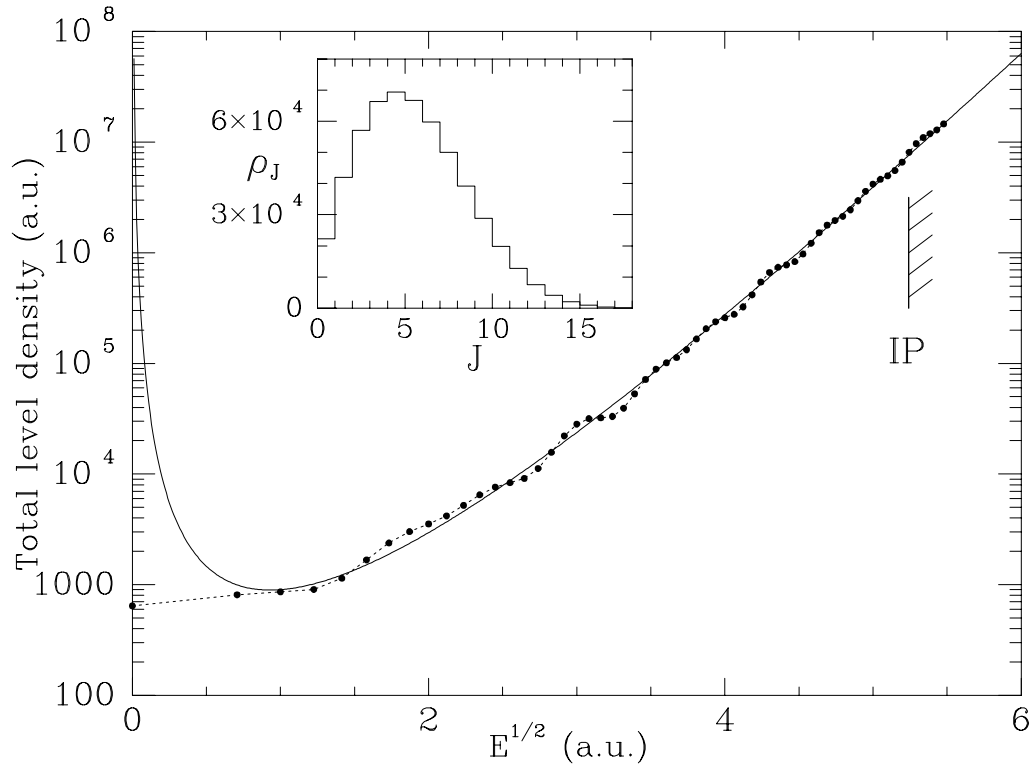


FIG. 2. Level density in  $\text{Au}^{24+}$ . Full circles – numerical calculation. Solid line – analytical fit, Eq. (3). The inset shows level densities at  $E \approx I$  for different  $J$ .



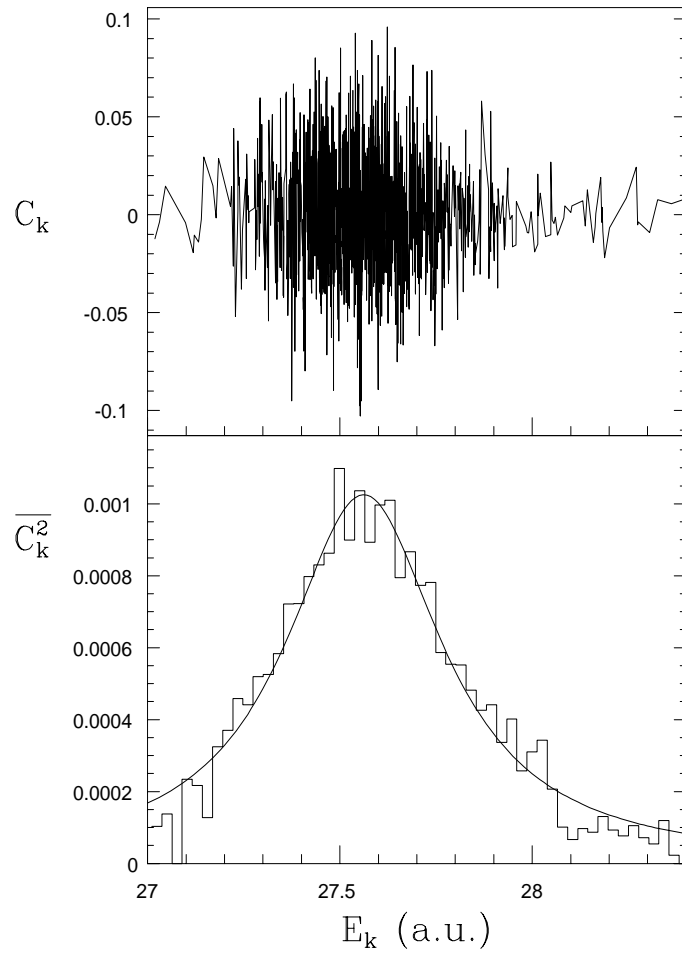


FIG. 3. Components of a 590th  $J^\pi = \frac{13}{2}^+$  eigenstate from a two-configuration calculation (top), and a fit of  $\overline{C_k^2}(E)$  by the Breit-Wigner formula (bottom).

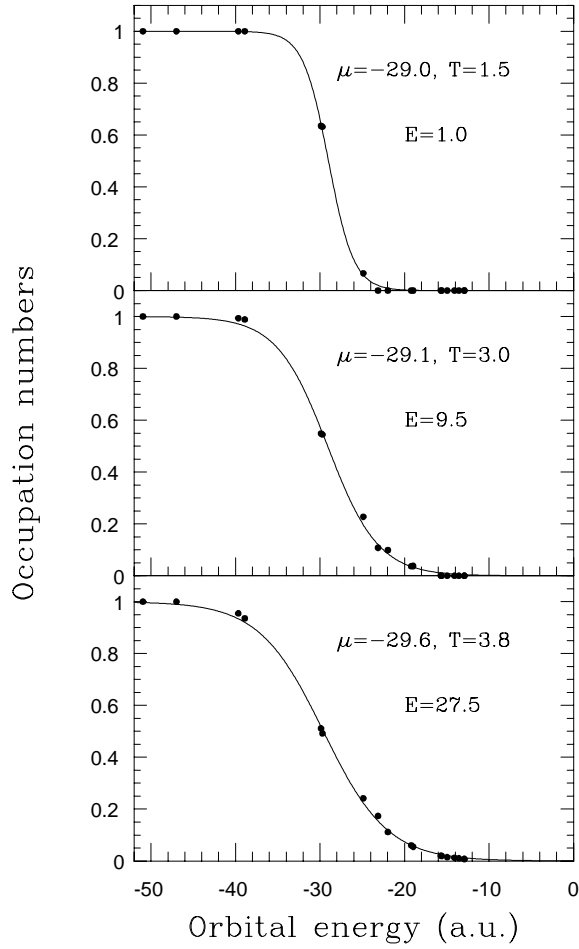


FIG. 4. Orbital occupation numbers in  $\text{Au}^{24+}$  calculated at  $E = 1, 9.5,$  and  $27.5$  a.u. (circles), compared with the Fermi-Dirac distribution (solid line).

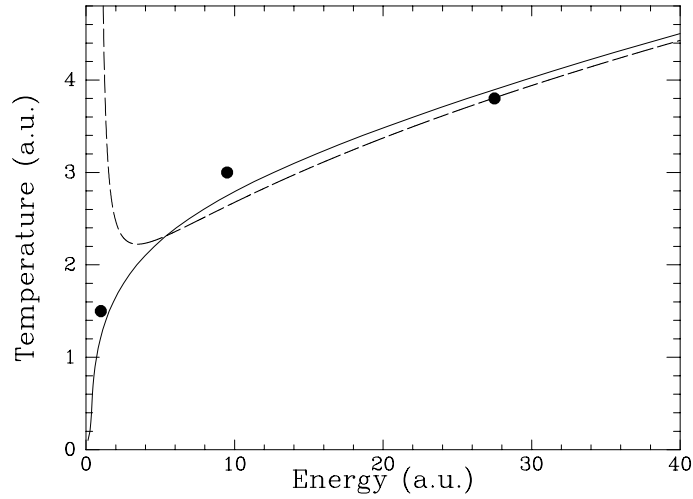


FIG. 5. Temperature vs energy for  $\text{Au}^{24+}$ . Solid line - canonical definition; dashed line - statistical definition; solid circles - Fermi-Dirac fits of the occupation numbers.